Cellular Physiology and Biochemistry

Cell Physiol Biochem 2017;42:506-518
DOI: 10.1159/000477597
Published online: June 02, 2017
Accepted: January 10, 2017

Original Paper

Protective Effects of MicroRNA-126 on Human Cardiac Microvascular Endothelial Cells Against Hypoxia/Reoxygenation-Induced Injury and Inflammatory Response by Activating PI3K/Akt/eNOS Signaling Pathway

Hong-Hui Yang[a] Yan Chen[a] Chuan-Yu Gao[a] Zhen-Tian Cui[b] Jian-Min Yao[b]

[a]Department of Cardiology, Zhengzhou University People's Hospital, Zhengzhou, [b]Cardiovascular Surgery, General Hospital of Beijing Military Region, Chinese People's Liberation Army, Beijing, P. R. China

Key Words
MicroRNA-126 • PI3K • Akt • eNOS • Human cardiac microvascular endothelial cells • Inflammatory response

Abstract
Objective: This study explored the protective effects of the microRNA-126 (miR-126)-mediated PI3K/Akt/eNOS signaling pathway on human cardiac microvascular endothelial cells (HCMECs) against hypoxia/reoxygenation (H/R)-induced injury and the inflammatory response. ***Methods:*** Untreated HCMECs were selected for the control group. After H/R treatment and cell transfection, the HCMECs were assigned to the H/R, miR-126 mimic, mimic-negative control (NC), miR-126 inhibitor, inhibitor-NC, wortmannin (an inhibitor of PI3K) and miR-126 mimic + wortmannin groups. Super oxide dismutase (SOD), nitric oxide (NO), vascular endothelial growth factor (VEGF) and reactive oxygen species (ROS) were measured utilizing commercial kits. Quantitative real-time polymerase chain reaction (qRT-PCR) and enzyme-linked immunosorbent assay (ELISA) were performed to detect miR-126 expression and the mRNA and protein expression of inflammatory factors. Western blotting was used to determine the expression of key members in the PI3K/Akt/eNOS signaling pathway. ACCK-8 assay and flow cytometry were employed to examine cell proliferation and apoptosis, respectively. The angiogenic ability in each group was detected by the lumen formation test. ***Results:*** Compared to the control group, p/t-PI3K, p/t-Akt and p/t-eNOS expression, NO, VEGF and SOD levels, cell proliferation and *in vitro* lumen formation ability were decreased, while the ROS content, interleukin (IL)-6, IL-10 and tumor necrosis factor (TNF)-α expression and cell apoptosis were significantly increased in the H/R, mimic-NC, miR-126 inhibitor, inhibitor-NC, wortmannin and miR-126 mimic + wortmannin groups. Additionally, in comparison with the H/R group, the miR-126 mimic group had elevated p/t-PI3K, p/t-Akt and p/t-eNOS

Dr. Hong-Hui Yang
Department of Cardiology, Zhengzhou University People's Hospital, No.7, Weiwu Road, Zhengzhou 450001, Henan Province (P. R. China)
Tel./Fax +86-0371-87160315, E-Mail y_honghui@126.com

expression, increased NO, VEGF and SOD contents, and strengthened cell proliferation and lumen formation abilities but also exhibited decreased ROS content, reduced IL-6, IL-10 and TNF-α expressions, and weakened cell apoptosis, while the miR-126 inhibitor and wortmannin group exhibited the opposite results. Furthermore, decreased p/t-PI3K, p/t-Akt and p/t-eNOS expressions, decreased NO, VEGF and SOD contents, cell proliferation and lumen formation abilities, as well as increased ROS content, increased IL-6, IL-10 and TNF-α expression, and increased cell apoptosis were observed in the miR-126 mimic + wortmannin group compared to themiR-126 mimic group. ***Conclusions:*** These findings indicated that miR-126 protects HCMECs from H/R-induced injury and inflammatory response by activating the PI3K/Akt/eNOS signaling pathway.

Introduction

Human umbilical vein endothelial cells (HUVECs) are considered a common cell model for exploring the pathogenesis of cardiovascular disease and are essential in vascular physiology and pathology [1, 2]. Cardiac microvascular endothelial cells (CMECs), which exhibits pindle-shaped, polygonal-shaped, and typical cobblestone-like morphology, play leading roles in myocardial angiogenesis and have different structures and functions from HUVECs; the communication between CMECs and the surrounding cardiac myocytes regulates endothelial cell proliferation and angiogenesis [3, 4]. The cardiac microvasculature is located at the terminal end of the circulation, which determines the level of myocardial perfusion and the coronary reserve [3]. Being the most common cells in a normal heart, CMECs are a basic component of the myocardial microcirculation and play a key role in the preservation of cardiomyocytes (CMs) against reperfusion injury [5]. Sustained high levels of deleterious circulatory stimulation are associated with cardiovascular risk factors, including the diabetes-induced responses of vascular endothelial cells (ECs), which lead to a number of cardiovascular and cerebrovascular diseases (CCVD) and endothelial dysfunction [6]. Endothelial barrier dysfunction is considered one of the initiating mechanisms of diabetic microvascular complications, and characteristic changes include auto-regulatory dysfunction and increased endothelial permeability, all of which could help aggravate microvascular lesions and abnormal extravasations of inflammatory factors [7]. However, the inner mechanisms on the injury of vascular endothelial cells have not been illustrated clearly.

Being one of the small RNAs, microRNAs (miRs) are 21-25 nucleotides in length inherent in eukaryotic organisms, and their abnormal expression is closely associated with disease occurrence and development [8]. MiR-126 is the most commonly expressed miR in endothelial cells, including in the heart, lung and other murine tissues [9]. In addition, it can promote the invasion and metastasis of cancer cells by different mechanisms and inhibit angiogenesis and lung metastatic colonization in the human breast cancer MDA-MB-231 cells [10]. Previous studies have demonstrated that miRNAs could regulate CMECs-induced angiogenesis [11] and combinatorial microRNAs might inhibit hypoxia-induced cardiomyocytes apoptosis [12]. Endothelial nitric oxide synthase (eNOS) plays an important role in the regulation of vascular function and can produce nitric oxide (NO) and superoxide dismutase [13]. Previous investigations have demonstrated that the phosphatidylinositol-3 kinase/serine/threonine kinase (PI3K/Akt) signaling pathway is essential for regulating various cellular and molecular functions [14-16]. And Roundabout4 (Robo 4) could inhibit glioma-induced endothelial cell proliferation, migration and tube formation *in vitro* via the inhibition of VEGR2-mediated PI3K/AKT and FAK signaling pathways [17]. In addition, the growth factors and hormones of the PI3K/Akt pathway and eNOS activity could promote the survival of a variety of cells [18]. It has been verified that over-expression of miR-126 can block the activation of PI3K/Akt, leading to ischemic angiogenesis and tumor growth inhibition [9]. Therefore, we aimed to study the inner mechanism of miR-126 in the treatment of endothelial cell injury by regulating the PI3K/Akt/eNOS pathway.

Materials and Methods

Establishment of hypoxia and reoxygenation (H/R) model

The primary human cardiac microvascular endothelial cells (HCMEC, ScienCell™ Research Laboratories, Carlsbad, California, USA) were cultured with 10% heat-inactivated fetal bovine serum (FBS, Gibco Laboratories, Grand Island, New York, USA) and extracellular matrix (EMC, HyClone Laboratories, Logan, Utah, USA) culture solution containing with 100 units/mL penicillin/streptomycin (HyClone Laboratories, Logan, Utah, USA) in a 5% CO_2 constant-temperature incubator at 37°C. The transfected cells were blocked by culturing for 4 h without serum. Then, 10% FBS was added and the cells were cultured for another 24 h. After that, the cells were placed in the anoxic tank at 37°C and closely monitored during 2 h of culture to induce hypoxia. Then, the cells were placed in the normoxic incubator for 24 h to allow re-oxygenation, and then they were collected for the subsequent experiments.

Cell culture, grouping and transfection

According to the damage H/R model of endothelial cells, this experiment was divided into 8 groups: the control group, the H/R group (exposed to H/R), the miR-126 mimic group (miR-126 mimic+ H/R), the mimic-negative control (NC) group (mimic-NC + H/R), the miR-126 inhibitor group (miR-126 inhibitor + H/R), the inhibitor-NC group (inhibitor-NC + H/R), wortmannin group (PI3K inhibitor + H/R) and the miR-126 mimic + wortmannin group (miR-126 mimic, PI3K inhibitor + H/R). The oligonucleotide sequences was shown in Table 1 and synthesized by the Shanghai GenePharma Co., Ltd. (Shanghai, China). The transfected mixtures were configured according to the instructions of the Lipofectamine 2000 (Invitrogen Inc., Carlsbad, California, USA) kit. The control and H/R groups were administered only culture medium without serum and double antibody. The wortmannin group and miR-126 mimic +wortmannin group both were administered50nmol/L of PI3K inhibitor wortmannin (Sigma-Aldrich Chemical Company, St Louis, Missouri, USA). The other groups were treated with liposome (Invitrogen Inc., Carlsbad, California, USA) encapsulated oligonucleotide medium (final concentration of 20μmol/L).

Quantitative real-time polymerase chain reaction (qRT-PCR)

The miRNA was extracted according to the instructions of the miRNeasy Mini kit (Qiagen company, Hilden, Germany), and total RNA was extracted according to the instructions for TRIzol (Invitrogen Inc., Carlsbad, California, USA). The RNA concentration was detected by NanoDrop2000 (Thermo Fisher Scientific Inc., Waltham, Massachusetts, USA) and stored at -80°C for further use. According to the gene sequence published in the GenBank database, primers were designed with Primer 5.0 design software (Table 2) and they were synthetized by the Shanghai GenePharma Co., Ltd. (Shanghai, China). The miRNA reverse transcription was carried out with the One Step PrimeScript® miRNA cDNA Synthesis Kit (Perfect Real Time) (Takara Holdings Inc., Kyoto, Japan). The miRNA was reacted at 37°C for 1 h (poly (A) tail addition and reverse transcription reaction) and then heat shocked at 85°C for 5 s (enzyme inactivation reaction). The qRT-PCR reaction conditions for miRNA were as follows: 42°C for 5 min, 95°C for 10 s, and then 40 cycles of 95°C for 5 s, 60°C for 1 min and 72°C for 15 s. The qRT-PCR of non-miRNA was performed according to the instructions of One Step SYBR® PrimeScript® PLUS RT- PCR Kit (Takara Holdings Inc., Kyoto, Japan). The PCR reaction conditions were as follows: 42°C for 5 min, 95°C for 10 s, and then 40 cycles of 94°C for 5 s, 58°C for 30 s, 72°C for 15 s. U6/β-actin was used as the internal reference, and the reliability of the PCR results was evaluated by the dissolution curve. The Ct value (power curve of amplification), ΔCt = Ct (target gene) – Ct (reference), ΔΔCt = ΔCt (the experimental group) - ΔCt (the control group). And the relative expression of the target gene was calculated according to $2^{-\Delta\Delta Ct}$ [19].

Table 1. The oligonucleotide sequences. Note: miR-126, microRNA-126; NC: negative control

Group	Sequence
miR-126 mimic	5'-UCGUACCGUGAGUAAUAAUGCG-3'
mimic-NC	5'- UUCUCCGAACGUGUCACGUTT-3'
miR-126 inhibitor	5'- CGCAUUAUUACUCACGGUACGA-3'
inhibitor-NC	5'- CAGUACUUUUGUGUAGUACAA-3'

Table 2. Primers of miRNA and inflammatory factors. Note: miR-126, microRNA-126; IL, interleukin; TNF-α, tumor necrosis factor-α

Gene		Primer sequence
miR-126	RT primer	5'-GTCGTATCCAGTGCGTGTCGTGGAGTCGGCAATTGCACTGGATACGACCGCATTA-3'
U6	RT primer	5'-CGCTTCACGAATTTGCGTGTCAT-3'
miR-126	Forward primer	5'-AGTGCAGGGTCCGAGGTAT-3'
	Reverse primer	5'-GCCGCTCGTACCGTGAGTAATAATG-3'
U6	Forward primer	5'-CTCGCTTCGGCAGCACA-3'
	Reverse primer	5'-AACGCTTCACGAATTTGCGT-3'
IL-6	Forward primer	5'-AGGATACCACTCCCAACAGACCT-3'
	Reverse primer	5'-CAAGTGCATCATCGTTGTTCATAC-3'
IL-10	Forward primer	5'-TTACCTGGAGGAGGTGATGC-3'
	Reverse primer	5'-TGGGGGTTGAGGTATCAGAG-3'
TNF-α	Forward primer	5'-CTTCTCCTTCCTGATCGTGG-3'
	Reverse primer	5'-GCTGGTTATCTCTCAGCTCCA-3'
β-actin	Forward primer	5'-CCTGGGCATGGAGTCCTGTG-3'
	Reverse primer	5'-AGGGGCCGGACTCGTCATAC-3'

Detection of SOD activity and the levels of NO, VEGF and ROS

The SOD detection kit was provided by the JianCheng biological company (Nanjing, Jiangsu Province, China). The reaction solution was configured according to the instructions. After mixing evenly, the reaction solution was incubated at room temperature for 10 min. A Type 722 spectrophotometer (Thermo Fisher Scientific, Waltham, MA, USA) was used to detect the optical density (OD) at the wavelength of 550 nm. The SOD activity (U/mL) = (control tube $_{OD}$– determination tube $_{OD}$)/control tube $_{OD}$/50%.

The relative concentration of nitric oxide (NO) was detected as follows: 1 mL of sample was added to 0.5 mL 0.02% 4-hydroxycoumarin (solubilized in dimethylformamide: 2 mol/L HCl, 1: 1 volume ratio, Sigma-Aldrich Chemical Company, St Louis, Missouri, USA). The sample was incubated on ice for 5min after being mixed evenly and was added to 50 μl 8% $Na_2S_2O_3$ (Sigma-Aldrich Chemical Company, St Louis, Missouri, USA) and allowed to sit for 10 min at room temperature. Then, 0.5 mL 1.5 mol/L NaOH (Sigma-Aldrich Chemical Company, St Louis, Missouri, USA) was added and the solution stood for 10 min at room temperature. The relative fluorescence intensity was detected by Thermo fluorescence spectrophotometer. The standard curve was drawn based on the standard $NaNO_2$ (Sigma-Aldrich Chemical Company, St Louis, Missouri, USA) and the relative concentration of NO was calculated.

The detection process strictly complied with the vascular endothelial growth factor (VEGF) ELISA Kit (Roche Ltd., Basel, Switzerland) instructions. The ELISA kit was allowed to sit for 20 min at room temperature and then the washing liquid, standard products and reaction system were configured. The OD value of each well (450 nm) was detected after addition of the Universal enzyme marker (BioTek Synergy 2) 3 min after the liquid reaction was terminated. The standard curve was drawn based on the OD value, and the content of VEGF was calculated.

An intracellular oxidation activated oxygen fluorescence assay kit (GENMED SCIENTIFICS INC., Arlington, Massachusetts, USA) was adopted to detect the content of reactive oxygen species (ROS). When the cells reached 70% confluence, the medium was removed and GENMED staining solution and diluent solution were added to the cell culture plate. The cells were incubated at 37°C for 20 min. After that, the GENMED staining solution was aspirated, and 500 μl pre-heated GENMED preservation solution was added to the cell culture wells. The fluorescence value was observed through the cell culture well by the fluorescence spectrophotometer when the emission wavelength was set at 590 nm and the excitation wavelength at 540 nm. The relative content of ROS was calculated based on the standard curve.

Enzyme-linked immunosorbent assay (ELISA)

The detection process strictly complied with the ELISA Kit (Bio-Rad, Inc., Hercules, California, USA) instructions. The ELISA Kit was allowed to sit at room temperature for 20 min and then the washing liquid was prepared. After the standard sample was dissolved, 100 μl mixture was added to the reaction plate to generate the standard curve. The 100 μl sample was added to the reaction well and incubated at 37°C for 90 min. The 100μl working fluid with biotin antibody was added to the sample solution after washing and incubated at 37°C for 60 min. After washing, the 100μl working fluid with enzyme binding reaction (protected from light) was added and incubated at 37°C for 60 min. The culture plate was washed 3 times and added to 100μl substrate. After incubating for 15 min at 37°C in the dark, the terminating fluid was

quickly added to stop the reaction. The Universal enzyme marker (BioTek Synergy 2) was applied to detect the OD values of each tube at 450 nm within 3 min. According to the OD values, the standard curve was drawn and the contents of interleukin-6 (IL-6), IL-10 and tumor necrosis factor-α (TNF-α) in the cell supernatant of each group were analyzed.

Western blotting

The concentration of extracted protein was determined by BCA Kit (Wuhan Boster Biological Technology Co., Ltd., Wuhan, Hubei Province, China). The extracted protein was added to the sample buffer and boiled at 95°C for 10 min, followed by the addition of 50 μg sample in each well. After that, 10% polyacrylamide gel (Wuhan Boster Biological Technology Co., Ltd., Wuhan, Hubei Province, China) electrophoresis was carried out to isolate the protein. The electrophoresis voltage was changed from 80 V to 120 V, and wet transfer with transfer voltage of 100 mV continued for 70 min to transfer the proteins to PVDF membrane. Then, the membranes were blocked with 5% BSA at room temperature for 1h, followed by the addition of primary antibodies (p-AKT (ab81283), t-AKT (ab179463), p-PI3K (ab182651), t-PI3K (ab86714), p-eNOS (ab76199), eNOS (ab66127) and β-actin (ab8226) (all at a1:1000 dilution, Abcam Inc., Cambridge, Massachusetts, USA) and incubation overnight at 4°C. Tris-buffered saline Tween-20 (TBST) was used to wash the membranes 3 times for 5 min each, and the corresponding secondary antibody (at a 1: 1000 dilution, Abcam Inc., Cambridge, Massachusetts, USA) was added and incubated at room temperature for 1 h, followed by a membrane wash at 3 times/5 min. The Roche ECL chemiluminescence reagent was applied for band development. The β-actin was used as an internal reference, and Bio-rad Gel Dol EZimaging (GEL DOC EZ IMAGER, Bio-rad, Hercules, California, USA) was used for image analysis. Image J software was adopted to analyzed the grey value for the target bands.

CCK-8 assay

The cells were inoculated into 96-well plates (100μl cell suspension, 5000 cells per well). After transfection, the cells were cultured for 24 h, and the cell proliferation was detected by cell counting kit-8 (CCK-8) (Beyotime Institute of Biotechnology, Haimen, Jiangsu Province, China). According to the kit instructions, the cell plates were removed, and 10μl CCK-8 reagent was added to each well. Then, the cells were incubated for 3 h at 37°C.The OD at 450 nm in each well was detected by the multifunctional enzyme standard instrument (Thermo Fisher Scientific, Waltham, MA, USA). In the experiment, the concentration of DMSO in each well was no more than 0.1%, and 4 duplicated wells were set. The above actions were repeated 3 times, and the average value was calculated. The rate of miR-126 cell proliferation was calculated according to the OD value of each well. The cell viability (%) of each group was detected at different time points and it was used as a testing index. Cell proliferation activity (%) = $(OD_{\text{experimental group}} - OD_{\text{blank control group}})/(OD_{\text{control group}} - OD_{\text{blank control group}}) \times 100\%$.

Flow cytometry

The apoptosis rate was detected by an Annexin V FITC apoptosis kit. The transfected cells were digested by 2.5% trypsin and centrifugation at 1000 r/min for 5 min with supernatant discarded. The suspended in buffer solution (PBS with calcium) for the preparation of a single cell suspension with 1×10^6 cell/ml concentration. At room temperature, the 100μl cell suspension was placed into the test tube. Propidium iodide (PI) and RNase A with the same final concentration of 10mg/mL were added and mixed in the tube, followed by incubation at 4°C for 30 min. After 400μl staining buffer was added, the cells were immediately detected and analyzed with flow cytometry (Becton, Dickinson and Company, Franklin Lakes, New Jersey, USA). A total of 10^4 cells were selected each time, and Cell Quest software was utilized to conduct data analysis. Annexin V-positive cells were apoptotic cells, and the right upper quadrant and the right lower quadrant presented the apoptotic cells. The cell apoptosis rates of each group were calculated.

In vitro lumen formation assay

The pre-liquefied matrigel (BD Company) was added (60 μl) to a sterilized 96-well plate (Corning Glass Works, Corning, New York, USA) and was evenly distributed in each well of the culture plate. The 96-well plate was then placed in the incubator at 37°C for 30min and removed after matrigel coagulation. To each well, 100 μl of transfected cells in logarithmic growth was added at a density of 1×10^5 cell/mL, and then the cells were cultured in a 5% CO_2 constant temperature incubator at 37°C. After incubation for 24 h, the

transfected cells were placed under a phase-contrast microscope (Olympus Optical Co., Ltd, Tokyo, Japan) to observe the changes in lumen formation ability of the cells in each group. The lumen formation ability was observed by photos under high magnification (400 ×).

Statistical analysis

All data were analyzed with SPSS 21.0 statistical software (SPSS, Inc., Chicago, Illinois, USA). The measurement data were expressed as the mean ± standard deviation. Independent-sample *t* test was applied in comparisons between two groups when the data obeyed a normal distribution and one-way analysis of variance (ANOVA) was used in comparisons among several groups. Count data was expressed by percentage or rate and tested by Chi square test. $P < 0.05$ indicated statistical significant.

Results

Comparison of the miR-126 expression in each group

The expression of miR-126 in each group was analyzed by qRT-PCR. The corresponding results indicated that, compared with the control group, the expression of miR-126 in the H/R, wortmannin, mimic-NC, miR-126 inhibitor and inhibitor-NC groups were all significantly reduced (all $P < 0.05$), while there was no significant difference in the miR-126 mimic group and miR-126 mimic + wortmannin group. In comparison with the H/R group, the expression of miR-126 in the miR-126 mimic group and miR-126 mimic + wortmannin group were significantly increased, while it was notably decreased in the miR-126 inhibitor group (both $P < 0.05$) (Fig. 1).

Comparisons of the expressions of PI3K/Akt/eNOS signaling pathway-related proteins in each group

Western blotting was used to detect the protein expressions of PI3K/Akt/eNOS signaling pathway-related proteins. The results indicated that, when compared with the control group, the expression of p/t-PI3K, p/t-Akt, p/t-eNOS in the H/R, wortmannin, mimic-NC, miR-126 mimic + wortmannin, miR-126 inhibitor and inhibitor-NC groups was significantly decreased (all $P < 0.05$) in all, while no significant difference was found in themiR-126 mimic group. When compared with the H/R group, the p/t-PI3K, p/t-Akt, p/t-eNOS expression was significantly increased in the miR-126 mimic group, while the expression was found to be decreased in the wortmannin and miR-126 inhibitor groups (all $P < 0.05$). In comparison with the miR-126 mimic group, the expression of p/t-PI3K, p/t-Akt, p/t-eNOS in the miR-126 mimic + wortmannin group was significantly reduced (all $P < 0.05$) (Fig. 2). These results suggested that miR-126 could activate the PI3K/Akt/eNOS signaling pathway.

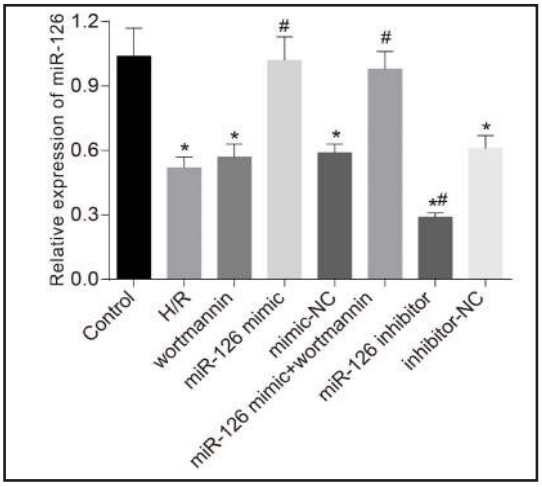

Fig. 1. Comparison of the miR-126 expression in each group. Note: *, $P < 0.05$, compared with the control group; #, $P < 0.05$, compared with the H/R group; miR-126, microRNA-126; H/R, hypoxia/reoxygenation; NC, negative control.

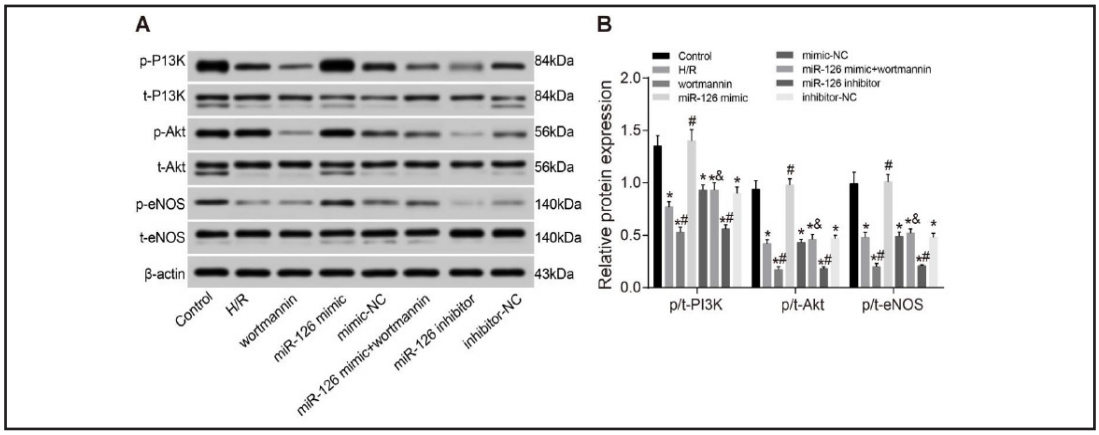

Fig. 2. Comparison of protein expressions of PI3K/Akt/eNOS signaling pathway-associated proteins in each group. (A: Western Blotting was applied to detect the protein expressions of PI3K/Akt/eNOS signaling pathway mediators in each group; B: The expressions of PI3K/Akt/eNOS signaling pathway mediators was analyzed by gray analysis). Note: *, $P < 0.05$, compared with the control group; #, $P < 0.05$, compared with the H/R group; &, $P < 0.05$, compared with the miR-126 mimic group; miR-126, microRNA-126; H/R, hypoxia/reoxygenation; NC, negative control.

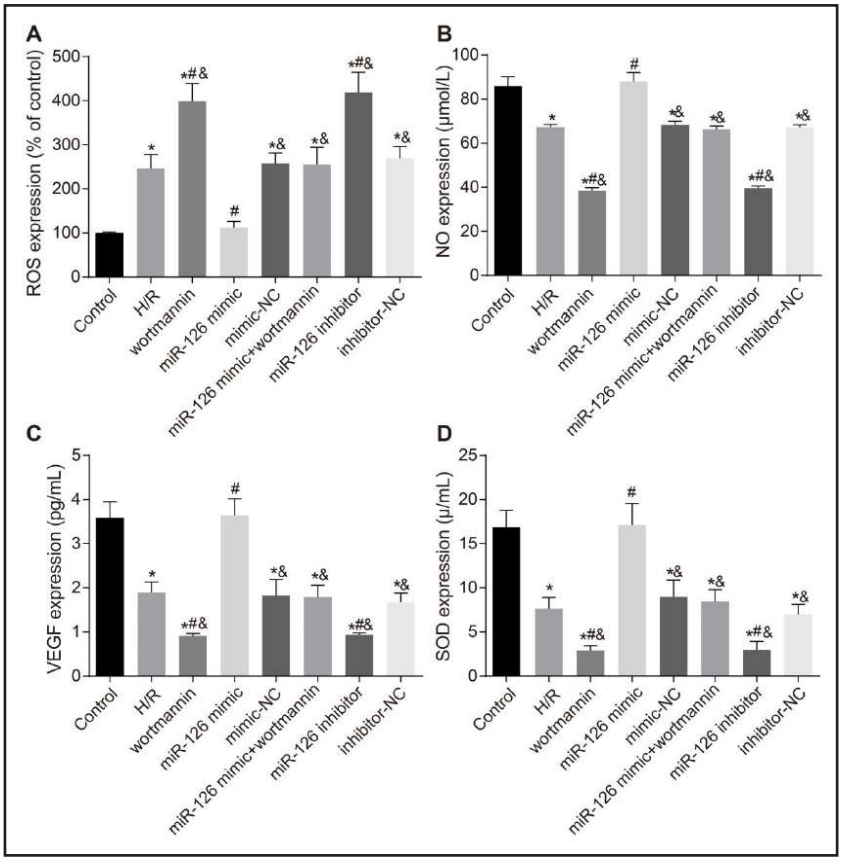

Fig. 3. Comparisons of SOD activity and the levels of NO, VEGF and ROS in each group (A: The expression of ROS in each group; B: The expression of NO in each group; C: The expression of VEGF expression in each group; D: The SOD activity in each group). Note: *, $P < 0.05$, compared with the control group; #, $P < 0.05$, compared with the H/R group; &, $P < 0.05$, compared with the miR-126 mimic group; miR-126, microRNA-126; H/R, hypoxia/reoxygenation; NC, negative control; ROS, reactive oxygen species; NO, nitric oxide; VEGF, vascular endothelial growth factor; SOD, super oxide dismutase.

Comparisons of SOD activity and the levels of NO, VEGF and ROS in each group

The expression of VEGF, SOD, NO and ROS was measured. Compared with the control group, the ROS expression in the H/R, wortmannin, mimic-NC, miR-126 mimic + wortmannin, MiR-126 inhibitor and inhibitor-NC groups was significantly elevated, while the expression of NO, VEGF and SOD was notably decreased(all $P < 0.05$). No obvious difference was found in the miR-126 mimic group. In addition, when compared with the H/R group, the expression

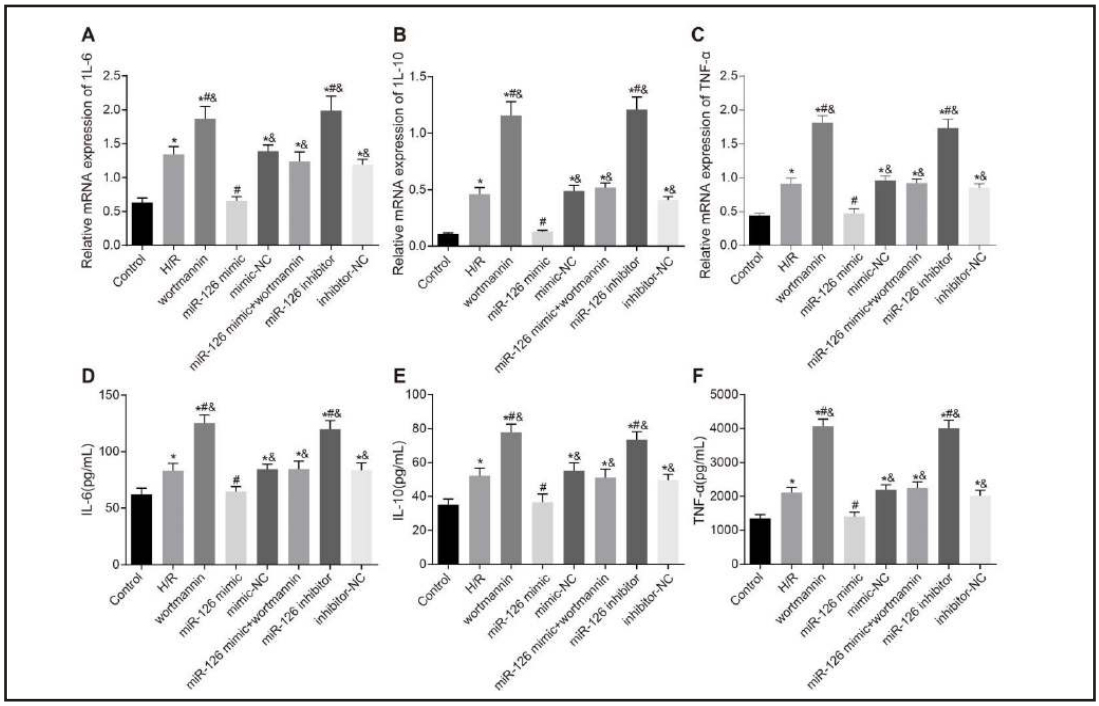

Fig. 4. Comparison of the expressions of inflammatory factors in each group (A: The expression of IL-6 mRNA in each group; B: The expression of IL-10 mRNA in each group; C: The expression of TNF-α mRNA in each group; D: Changes in the IL-6 level determined by ELISA in each group; E: Changes in the IL-10 level in each group; F: Changes in the TNF-α level detected by ELISA in each group). Note: *: $P < 0.05$, compared with the control group; #: $P < 0.05$, compared with the H/R group; &: $P < 0.05$, compared with the miR-126 mimic group; miR-126, microRNA-126; H/R: hypoxia/reoxygenation; NC: negative control; IL, interleukin; TNF-α, tumor necrosis factor-α; ELISA, enzyme-linked immunosorbent assay.

of ROS in the miR-126 mimic group was significantly decreased, while the expression of NO, VEGF and SOD was significantly increased; the expression of ROS in themiR-126 inhibitor group and wortmannin group was significantly increased, and the expression of NO, VEGF and SOD was significantly decreased (all $P < 0.05$). When compared with the miR-126 mimic group, the ROS expression in the miR-126 mimic + wortmannin group was significantly increased, while the NO, VEGF and SOD expression was significantly reduced (all $P < 0.05$) (Fig. 3). The above results suggested that miR-126 inhibits the down-regulation of the expression of NO, VEGF and SOD as well as the up-regulation of the expression of ROS induced by endothelial cell injury via the PI3K/Akt/eNOS signaling pathway.

Comparisons of the expressions of inflammatory factors in each group

The expression of inflammatory factors in each group was detected. When compared with the control group, the expression of mRNA and protein expression of IL-6, IL-10, TNF-α in the H/R,wortmannin, mimic-NC, miR-126 mimic + wortmannin, miR-126 inhibitor and inhibitor-NC groups were all significantly increased (all $P < 0.05$), and no obvious change of those inflammatory factors was found in the miR-126 mimic group. In comparison with the H/R group, the expression of IL-6, IL-10, TNF-α in the miR-126 mimic group was significantly reduced (which corresponded to the control group); the expression of IL-6, IL-10, TNF-α in themiR-126 inhibitor group was significantly elevated (all $P < 0.05$). The expression ofIL-6, IL-10, TNF-α in the miR-126 mimic + wortmannin group was significantly increased when compared with the miR-126 mimic group(all $P < 0.05$) (Fig. 4). These results demonstrated thatmiR-126 inhibits the up-regulation of the expression of IL-6, IL-10 and TNF-α-induced by endothelial cell injury via the PI3K/Akt/eNOS signaling pathway.

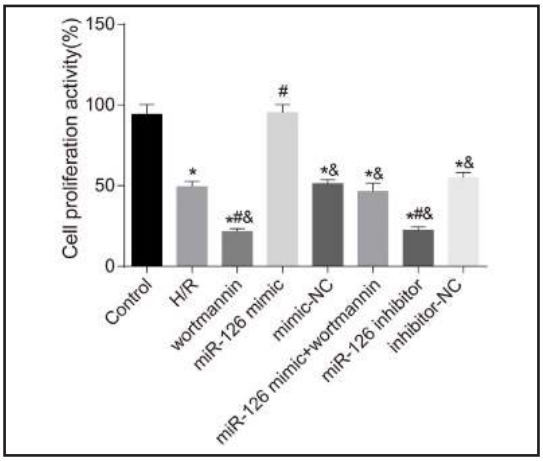

Fig. 5. Comparison of cell proliferation activity in each group. Note: *: $P < 0.05$, compared with the control group; #: $P < 0.05$, compared with the H/R group; &: $P < 0.05$, compared with the miR-126 mimic group; miR-126, microRNA-126; H/R: hypoxia/reoxygenation; NC: negative control.

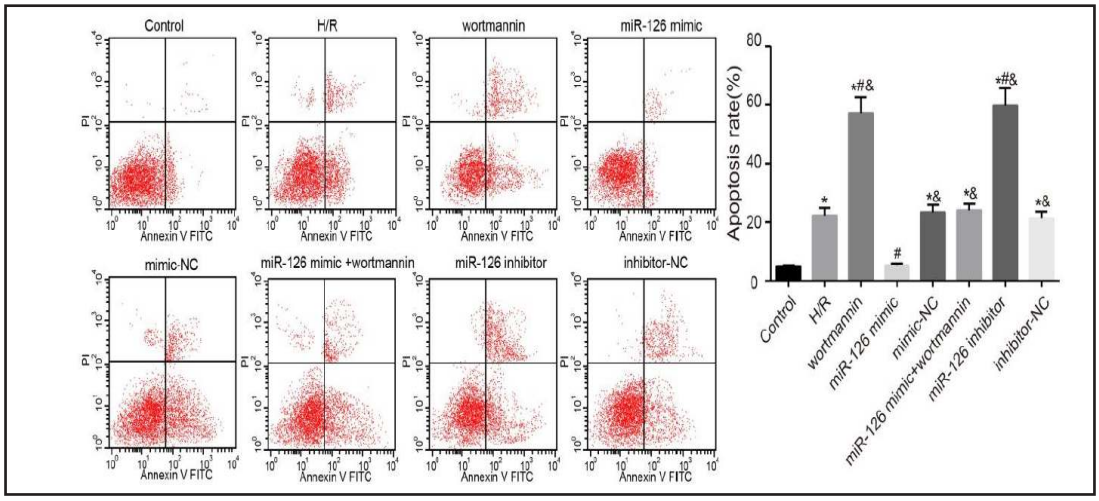

Fig. 6. Comparison of cell apoptosis in each group. Note: miR-126, microRNA-126; H/R: hypoxia/reoxygenation; NC: negative control;*: P < 0.05, compared with the control group; #: P < 0.05, compared with the H/R group; &: P < 0.05, compared with the miR-126 mimic group.

Effects of miR-126 on cell proliferation activity in each group

In comparison with the control group, the cell proliferation activity in the H/R, wortmannin, mimic-NC, miR-126 mimic + wortmannin, miR-126 inhibitor and inhibitor-NC groups was significantly diminished (all $P < 0.05$),while no obvious change was found in the miR-126 mimic group. When compared with the H/R group, the cell proliferation activity was significantly increased in themiR-126 mimic group while decreased in the miR-126 inhibitor and wortmannin groups(both $P < 0.05$). In comparison with the miR-126 mimic group, the cell proliferation activity in the miR-126 mimic + wortmannin was significantly diminished ($P < 0.05$) (Fig. 5). These results indicated that the decreased cell proliferation activity induced by endothelial cell injury could be alleviated by miR-126.

Effects of miR-126 on cell apoptosis in each group

A flow cytometry assay was applied to detect the effects of miR-126 on the cell apoptosis of CMECs. Compared with the control group, the cell apoptosis rates in the H/R, mimic-NC, miR-126 mimic + wortmannin, miR-126 inhibitor and inhibitor-NC groups were all significantly increased (all $P < 0.05$), while there was no obvious change in the miR-126 mimic group. In comparison with the H/R group, the cell apoptosis rate in the miR-126 mimic group was significantly decreased, reaching the normal level, while the cell apoptosis rates in the miR-126 inhibitor group and wortmannin group were significantly increased (both $P < 0.05$). When compared with the miR-126 mimic group, the cell apoptosis rate in

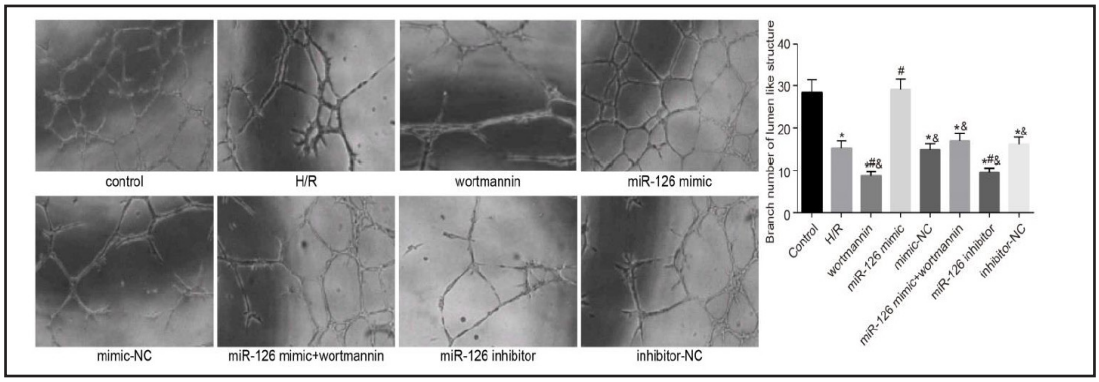

Fig. 7. Lumen formation determined by phase-contrast microscopy (400 ×). Note: *: $P < 0.05$, compared with the control group; #: $P < 0.05$, compared with the H/R group; &: $P < 0.05$, compared with the miR-126 mimic group; miR-126, microRNA-126; H/R, hypoxia/reoxygenation; NC, negative control.

the miR-126 mimic + wortmannin group was significantly elevated ($P < 0.05$) (Fig. 6). These results suggested that miR-126 inhibits the cell apoptosis induced by endothelial cell injury via the PI3K/Akt/eNOS signaling pathway.

Effects of miR-126 on in vitro lumen formation in each group

The relationship between miR-126 and angiogenesis was studied based on the *in vitro* lumen formation assay. The results suggested that lumen formation in the H/R, wortmannin, mimic-NC, miR-126 mimic + wortmannin, miR-126 inhibitor and inhibitor-NC groups were all significantly reduced in comparison with the control group(all $P < 0.05$), while no significant difference was found in the miR-126 mimic group. When compared with the H/R group, the lumen formation ability was significantly increased in the miR-126 mimic group, and it was significantly decreased in the miR-126 inhibitor group and wortmannin group (both $P < 0.05$). In comparison with the miR-126 mimic group, the lumen formation rate in themiR-126 mimic + wortmannin group was significantly reduced ($P < 0.05$) (Fig. 7). Altogether, these results demonstrated that the miR-126 could promote lumen formation after endothelial cell injury.

Discussion

As the most common cells in a normal human heart, CMECs play important roles with regard to myocardial protection during reperfusion injury by autocrine or paracrine secretion mechanisms [5]. OverexpressingmiR-126 could enhance ischemic angiogenesis due to stimulating the Akt/ERK–related pathway [20]. Therefore, our study aimed to explore the effects of miR-126 on relieving endothelial cell damage and inflammation via the PI3K/Akt/eNOS pathway.

The expression of miR-126wasdown-regulated in the H/R group, in which the activation of the PI3K/Akt/eNOS pathway was impaired, and the inflammatory response and cell apoptosis were also increased. Additionally, miR-126 could relieve cell proliferation activity and promote the lumen formation induced by endothelial cell injury. Endothelial cells are important in the regulation of vascular integrity and angiogenesis, and they mediate the development of miR-126 angiogenesis [21]. Additionally, the knockdown of miR-126 could cause loss of vascular integrity and hemorrhage, and the decreased expression of miR-223-3p also plays an essential role of angiogenesis in the CMECs of rats [22, 23]. The expression of miR-126 is essential for endothelial growth as a promoter for endothelial cell proliferation and migration, which makes it a putative tumor suppressor, in violation of intuition [24]. In addition, miR-126 is highly enriched in endothelial cells that produce the regulatory function in vascular integrity and vascular pathology [25]. MiR-126 has played significant

roles in different physiological and pathological processes, including inflammation, blood vessel growth, and cancer through various pathways [24]. Circulating miR-126-5p has been reported as an underlying biomarker for the complexity and severity of Coronary Artery Disease (CAD) in patients with stable angina pectoris [26]. Additionally, the effect of miR-126 on vascular inflammation is regulated by adhesion molecule-1 [27]. The way in which miR-126 affects endothelial cells is partially mediated by the PI3K/Akt/eNOS signaling pathway, of which PKB/Akt is significant in the apoptosis and survival of endothelial cells [28, 29]. Moreover, a previous study indicated that the expression of miR-126 could significantly improve the function of CD4+T cells *in vivo* and promote cell differentiation [30].

This study also suggested that miR-126 could activate the PI3K/Akt/eNOS signaling pathway to inhibit the down-regulated expression of VEGF and SOD and up-regulate the expression of IL-10 and TNF-α, which is motivated by endothelial cell injury. MiR-126 serves as a regulating and adjusting device in the control of PI3K-Akt pathway transduction, as the activation of the PI3K-Akt-pathway is activated by low expression of miR-126 [9]. Previous studies have proven that resveratrol could inhibit hydrogen peroxide-induced apoptosis in endothelial cells via the activation of PI3K/Akt by miR-126, and the overexpression of miR-126 could decrease PIK3R2 and enhance PKB/Akt [31, 32]. It has also reported that Selenium could inhibit homocysteine-induced dysfunction and apoptosis of endothelial cells by activating AKT pathway [33]. Additionally, eNOS reduction in endothelial cells is regulated by changes in the expression of miRNA [34]. In addition, endothelial cells respond to various proteins and growth factors that regulate angiogenesis [35]. VEGF is important for regulating the function of endothelial cells, in which miR-126 positively regulates the response of ECs to VEGF [36]. A previous study has indicated that miR-126 could regulate tumor angiogenesis, and the decreased expression of miR-126 is correlated with the increased mRNA and protein levels of VEGF-A, which indicated that the up-regulation of miR-126 reduced endothelial cell lumen formation ability and VEGF-induced migration [35]. In addition, miR-126 silencing could significantly down-regulate the expression of Foxp3 on Tregs accompanied by decreased expression of IL-10 [9]. In addition, the overexpression of miR-126 could reduce ROS production and TNF-α expression [37]. Another previous study illustrated that miR-126 could reduce vascular cell adhesion molecule 1 expression in ECs by combining with its 3' UTR, which could reduce leukocyte-EC interactions in response to TNF-α [38].

To sum up, this study noted that miR-126 could activate the PI3K/Akt/eNOS pathway to affect inflammation, cell apoptosis and activity, which has the potential to become a new target for the treatment of endothelial cell injury. However, more research should be performed to provide guidance for clinical treatment with respect to miR-126 and the PI3K/Akt/eNOS pathway for endothelial cell injury.

Acknowledgments

We would like to acknowledge the reviewers for their helpful comments on this paper.

Disclosure Statement

None.

References

1 Jia Y, Ji L, Zhang S, Xu L, Yin L, Li L, Zhao Y, Peng J: Total flavonoids from Rosa Laevigata Michx fruit attenuates hydrogen peroxide induced injury in human umbilical vein endothelial cells. Food Chem Toxicol 2012;50:3133-3141.

2 Zhu T, Yao Q, Hu X, Chen C, Yao H, Chao J: The Role of MCPIP1 in Ischemia/Reperfusion Injury-Induced HUVEC Migration and Apoptosis. Cell Physiol Biochem 2015;37:577-591.
3 Ge GH, Dou HJ, Yang SS, Ma JW, Cheng WB, Qiao ZY, Hou YM, Fang WY: Glucagon-like peptide-1 protects against cardiac microvascular endothelial cells injured by high glucose. Asian Pac J Trop Med 2015;8:73-78.
4 Li F, Yuan Y, Guo Y, Liu N, Jing D, Wang H, Guo W: Pulsed magnetic field accelerate proliferation and migration of cardiac microvascular endothelial cells. Bioelectromagnetics 2015;36:1-9.
5 Cui H, Li X, Li N, Qi K, Li Q, Jin C, Zhang Q, Jiang L, Yang Y: Induction of autophagy by Tongxinluo through the MEK/ERK pathway protects human cardiac microvascular endothelial cells from hypoxia/reoxygenation injury. J Cardiovasc Pharmacol 2014;64:180-190.
6 Mudau M, Genis A, Lochner A, Strijdom H: Endothelial dysfunction: the early predictor of atherosclerosis. Cardiovasc J Afr 2012;23:222-231.
7 Wei L, Sun D, Yin Z, Yuan Y, Hwang A, Zhang Y, Si R, Zhang R, Guo W, Cao F, Wang H: A PKC-beta inhibitor protects against cardiac microvascular ischemia reperfusion injury in diabetic rats. Apoptosis 2010;15:488-498.
8 Wu XB, Wang MY, Zhu HY, Tang SQ, You YD, Xie YQ: Overexpression of microRNA-21 and microRNA-126 in the patients of bronchial asthma. Int J Clin Exp Med 2014;7:1307-1312.
9 Qin A, Wen Z, Zhou Y, Li Y, Li Y, Luo J, Ren T, Xu L: MicroRNA-126 regulates the induction and function of CD4(+) Foxp3(+) regulatory T cells through PI3K/AKT pathway. J Cell Mol Med 2013;17:252-264.
10 Zhang Y, Yang P, Sun T, Li D, Xu X, Rui Y, Li C, Chong M, Ibrahim T, Mercatali L, Amadori D, Lu X, Xie D, Li QJ, Wang XF: miR-126 and miR-126* repress recruitment of mesenchymal stem cells and inflammatory monocytes to inhibit breast cancer metastasis. Nat Cell Biol 2013;15:284-294.
11 Dai GH, Ma PZ, Song XB, Liu N, Zhang T, Wu B: MicroRNA-223-3p inhibits the angiogenesis of ischemic cardiac microvascular endothelial cells via affecting RPS6KB1/hif-1a signal pathway. PLoS One 2014;9:e108468.
12 Xu Y, Zhu W, Wang Z, Yuan W, Sun Y, Liu H, Du Z: Combinatorial microRNAs suppress hypoxia-induced cardiomyocytes apoptosis. Cell Physiol Biochem 2015;37:921-932.
13 Forstermann U, Li H: Therapeutic effect of enhancing endothelial nitric oxide synthase (eNOS) expression and preventing eNOS uncoupling. Br J Pharmacol 2011;164:213-223.
14 Xing M: Genetic alterations in the phosphatidylinositol-3 kinase/Akt pathway in thyroid cancer. Thyroid 2010;20:697-706.
15 Dong R, Chen W, Feng W, Xia C, Hu D, Zhang Y, Yang Y, Wang DW, Xu X, Tu L: Exogenous Bradykinin Inhibits Tissue Factor Induction and Deep Vein Thrombosis via Activating the eNOS/Phosphoinositide 3-Kinase/Akt Signaling Pathway. Cell Physiol Biochem 2015;37:1592-1606.
16 Zhang Z, Zhang T, Zhou Y, Wei X, Zhu J, Zhang J, Wang C: Activated phosphatidylinositol 3-kinase/Akt inhibits the transition of endothelial progenitor cells to mesenchymal cells by regulating the forkhead box subgroup O-3a signaling. Cell Physiol Biochem 2015;35:1643-1653.
17 Cai H, Xue Y, Li Z, Hu Y, Wang Z, Liu W, Li Z, Liu Y: Roundabout4 suppresses glioma-induced endothelial cell proliferation, migration and tube formation in vitro by inhibiting VEGR2-mediated PI3K/AKT and FAK signaling pathways. Cell Physiol Biochem 2015;35:1689-1705.
18 Wang R, Peng L, Zhao J, Zhang L, Guo C, Zheng W, Chen H: Gardenamide A Protects RGC-5 Cells from H(2)O(2)-Induced Oxidative Stress Insults by Activating PI3K/Akt/eNOS Signaling Pathway. Int J Mol Sci 2015;16:22350-22367.
19 Tuo YL, Li XM, Luo J: Long noncoding RNA UCA1 modulates breast cancer cell growth and apoptosis through decreasing tumor suppressive miR-143. Eur Rev Med Pharmacol Sci 2015;19:3403-3411.
20 Chen JJ, Zhou SH: Mesenchymal stem cells overexpressing MiR-126 enhance ischemic angiogenesis via the AKT/ERK-related pathway. Cardiol J 2011;18:675-681.
21 Wang S, Aurora AB, Johnson BA, Qi X, McAnally J, Hill JA, Richardson JA, Bassel-Duby R, Olson EN: The endothelial-specific microRNA miR-126 governs vascular integrity and angiogenesis. Dev Cell 2008;15:261-271.
22 Fish JE, Santoro MM, Morton SU, Yu S, Yeh RF, Wythe JD, Ivey KN, Bruneau BG, Stainier DY, Srivastava D: miR-126 regulates angiogenic signaling and vascular integrity. Dev Cell 2008;15:272-284.
23 Dai GH, Liu N, Zhu JW, Yao J, Yang C, Ma PZ, Song XB: Qi-Shen-Yi-Qi Dripping Pills Promote Angiogenesis of Ischemic Cardiac Microvascular Endothelial Cells by Regulating MicroRNA-223-3p Expression. Evid Based Complement Alternat Med 2016;2016:5057328.

24 Meister J, Schmidt MH: miR-126 and miR-126*: new players in cancer. ScientificWorldJournal 2010;10:2090-2100.
25 Asgeirsdottir SA, van Solingen C, Kurniati NF, Zwiers PJ, Heeringa P, van Meurs M, Satchell SC, Saleem MA, Mathieson PW, Banas B, Kamps JA, Rabelink TJ, van Zonneveld AJ, Molema G: MicroRNA-126 contributes to renal microvascular heterogeneity of VCAM-1 protein expression in acute inflammation. Am J Physiol Renal Physiol 2012;302:F1630-1639.
26 Li HY, Zhao X, Liu YZ, Meng Z, Wang D, Yang F, Shi QW: Plasma MicroRNA-126-5p is Associated with the Complexity and Severity of Coronary Artery Disease in Patients with Stable Angina Pectoris. Cell Physiol Biochem 2016;39:837-846.
27 Harris TA, Yamakuchi M, Kondo M, Oettgen P, Lowenstein CJ: Ets-1 and Ets-2 regulate the expression of microRNA-126 in endothelial cells. Arterioscler Thromb Vasc Biol 2010;30:1990-1997.
28 Meng S, Cao JT, Zhang B, Zhou Q, Shen CX, Wang CQ: Downregulation of microRNA-126 in endothelial progenitor cells from diabetes patients, impairs their functional properties, via target gene Spred-1. J Mol Cell Cardiol 2012;53:64-72.
29 Almhanna K, Strosberg J, Malafa M: Targeting AKT protein kinase in gastric cancer. Anticancer Res 2011;31:4387-4392.
30 Cui P, Hu Y, Tao Y, Chen C, Zhao J, Guo M, Zhou Y, Xu L: [miR-126 knockdown enhances the activity of murine CD4+ T cells in vivo and promotes their differentiation into Th1 cells]. Xi Bao Yu Fen Zi Mian Yi Xue Za Zhi 2016;32:347-351.
31 Sui XQ, Xu ZM, Xie MB, Pei DA: Resveratrol inhibits hydrogen peroxide-induced apoptosis in endothelial cells via the activation of PI3K/Akt by miR-126. J Atheroscler Thromb 2014;21:108-118.
32 Wang J, Chen Y, Yang Y, Xiao X, Chen S, Zhang C, Jacobs B, Zhao B, Bihl J, Chen Y: Endothelial progenitor cells and neural progenitor cells synergistically protect cerebral endothelial cells from Hypoxia/reoxygenation-induced injury via activating the PI3K/Akt pathway. Mol Brain 2016;9:12.
33 Ren H, Mu J, Ma J, Gong J, Li J, Wang J, Gao T, Zhu P, Zheng S, Xie J, Yuan B: Selenium Inhibits Homocysteine-Induced Endothelial Dysfunction and Apoptosis via Activation of AKT. Cell Physiol Biochem 2016;38:871-882.
34 Rippe C, Blimline M, Magerko KA, Lawson BR, LaRocca TJ, Donato AJ, Seals DR: MicroRNA changes in human arterial endothelial cells with senescence: relation to apoptosis, eNOS and inflammation. Exp Gerontol 2012;47:45-51.
35 Wang L, Lee AY, Wigg JP, Peshavariya H, Liu P, Zhang H: miR-126 Regulation of Angiogenesis in Age-Related Macular Degeneration in CNV Mouse Model. Int J Mol Sci 2016;17:895.
36 Huang F, Fang ZF, Hu XQ, Tang L, Zhou SH, Huang JP: Overexpression of miR-126 promotes the differentiation of mesenchymal stem cells toward endothelial cells via activation of PI3K/Akt and MAPK/ERK pathways and release of paracrine factors. Biol Chem 2013;394:1223-1233.
37 Wang Y, Wang F, Wu Y, Zuo L, Zhang S, Zhou Q, Wei W, Wang Y, Zhu H: MicroRNA-126 attenuates palmitate-induced apoptosis by targeting TRAF7 in HUVECs. Mol Cell Biochem 2015;399:123-130.
38 Sun X, Belkin N, Feinberg MW: Endothelial microRNAs and atherosclerosis. Curr Atheroscler Rep 2013;15:372.